MAUSAM, **77**, 1(January 2026), 247-264

MAUSAM

DOI: https://doi.org/10.54302/17rh9b48
Homepage: https://mausamjournal.imd.gov.in/index.php/MAUSAM

UDC No. 633:551.573(540)

Projecting evapotranspiration pattern over lower Gangetic plains of India with special reference to pre-monsoon and post-monsoon seasons

ABHILASHAA DAS[1], SAON BANERJEE[2*], SARATHI SAHA[1]

[1]*Department of Agricultural Meteorology and Physics, Bidhan Chandra Krishi Viswavidyalaya, Mohanpur, Nadia- 741252*

[2]*Departrment of Agricultural Meteorology and Physics, Bidhan Chandra Krishi Viswavidyalaya, Mohanpur, Nadia- 741252*

(*Received 29 April 2024, Accepted 9 May 2025*)

***Corresponding author's email: sbaner2000@yahoo.com**

सार – पोटेंशियल इवेपोट्रांसपिरेशन (PET) और बारिश के पूर्वानुमान महत्वपूर्ण कारक हैं जो प्रभावी फसल योजना और प्रबंधन में अहम भूमिका निभाते हैं। इस अध्ययन में, भारत में लोअर गैंगेटिक प्लेन (LGP) के भविष्य के PET और इफेक्टिव रेनफॉल (ER) में बदलाव का मूल्यांकन करने के लिए तीन ग्लोबल सर्कुलेशन मॉडल (GCMs) के मिले-जुले परिणामों का इस्तेमाल किया गया। यह मूल्यांकन दो समय अवधियों के लिए किया गया: मध्य-शताब्दी (2030-2040) और सदी के आखिर (2070-2090) के लिए, दो रिप्रेजेंटेटिव कंसंट्रेशन पाथवे (RCP) सिनेरियो (RCP 4.5 और RCP 8.5) का उपयोग करके। जलवायु अनुमानों को डाउनस्केल करने के लिए MarkSim DSSAT वेदर फ़ाइल जेनरेटर का इस्तेमाल किया गया। मॉडल द्वारा सिम्युलेट किए गए तापमान, सौर विकिरण और बारिश में सदी के दौरान मुख्य रूप से वृद्धि हुई, जिसमें दशक के हिसाब से थोड़ा बदलाव हुआ। सभी स्टेशनों के लिए कुल PET में RCP 4.5 के तहत 2030-2050 के लिए 2.02 mm प्रति वर्ष और 2070-2090 के लिए 0.88 mm प्रति वर्ष की दर से वृद्धि होने का अनुमान है। RCP 8.5 के तहत, यही दर 2030-2050 के लिए 2.29 mm प्रति वर्ष और 2070-2090 के लिए 3.02 mm प्रति वर्ष जितनी अधिक है। सबसे अधिक मासिक PET मई में दर्ज किया गया। दशकों के भीतर बारिश में बड़े बदलाव के बावजूद, RCP 4.5 ने कुल मिलाकर बढ़ती प्रवृत्ति (लगभग 5.5%) दिखाई, जबकि RCP 8.5 ने घटती प्रवृत्ति दिखाई। कल्याणी (नया जलोढ़ क्षेत्र) ने अन्य स्टेशनों की तुलना में सदी के आखिर तक (RCP 8.5) PET में सबसे अधिक गिरावट (22.38%) दिखाई। अनुमानित समय सीमा में, "ER - PET" का मान कम हो जाएगा, जो सिंचाई के पानी की उच्च मांग को दर्शाता है। परिणामों ने इष्टतम उत्पादन का समर्थन करने के लिए फसलों की आर्थिक योजना में मूल्यवान जानकारी प्रदान की।

ABSTRACT. Future predictions of potential evapotranspiration (PET) and rainfall are important factors that play pivotal role in effective crop planning and management. In this study, ensembled results of three Global Circulation Models (GCMs) were used to evaluate the changes in future PET and effective rainfall (ER) of the Lower Gangetic Plain (LGP) in India for two time slices: mid-century (2030-2040) and late-century (2070-2090) using two Representative Concentration Pathway (RCP) scenarios (RCP 4.5 and RCP 8.5). The MarkSim DSSAT Weather File Generator was used to downscale the climate projections. Temperatures, solar radiation, and rainfall simulated by the model majorly increased over the century, with slight decadal variations. The ensemble total PET for all stations combined has been projected to increase at the rate of 2.02 mm per year for 2030-2050 and 0.88 mm per year for 2070 – 2090 under RCP 4.5. Under RCP 8.5, the same is as high as 2.29 mm per year for 2030 - 2050 and 3.02 mm per year for 2070-2090. The highest monthly PET is recorded in May. Despite large variation in rainfall within decades, RCP 4.5 showed an overall increasing trend (approximately 5.5%), whereas RCP 8.5 showed a decreasing trend. Kalyani (New alluvial zone) demonstrated maximum decline in PET (22.38%) by late century (RCP 8.5) compared to other stations. Over the projected timeframe, "ER - PET" value will decrease, indicating a high demand for irrigation water. The results provided valuable insights into the economic planning of crops to support optimum production.

Key words – Climate change, Hydrologic projection, MarkSim weather generator, GCMs, RCPs.

1. Introduction

Agricultural production is estimated to expand approximately by 70% by 2050 with the ever-growing population (World Bank, 2020) Water in Agriculture (worldbank.org). The future projection of climate change as reported by the 6th Intergovernmental Panel on Climate Change (IPCC) assessment indicates that the average earth's temperature will escalate by 1.5 °C or more by the next 20 years. It has been predicted that by 2025, an estimated 1.8 billion people will live in areas with water scarcity; 66% of the global population residing in water-constrained regions (Hinrichsen and Tacio, 2002). According to a projection made by Seametrics, India, with its rising population, is expected to reach a water demand of 1.5 trillion cubic meters by 2030. A 40% depravity in water is predicted by 2030, if the current rate of water usage is not monitored. Water management and sustainability are, therefore, a top priority of concerned organizations.

The Lower Gangetic Plains is one of the most densely populated areas in India where agriculture serves as a major source of income. Irrigation doubles crop production per unit of land compared to rainfed farming, promoting both crop diversification and intensification (World Bank, 2020). Estimation of evapotranspiration and crop water requirements assist in successful planning of irrigation projects. Rainfall, temperature, and evapotranspiration are major parameters controlling climate change. Understanding long term evapotranspiration and rainfall pattern will help in better management of crop production (Idso *et al*., 1975; Su, 2002) by predicting irrigation requirements and thereby regulating crop water demand. PET serves as a vital input in planning crop water requirement and hydrological models (Allen *et al*., 1998). Predominant cropping systems followed in LGP are Rice-Rice, Rice-Wheat, Jute-Wheat, Jute-Pulses-Rapeseed, Jute-Rapeseed-Rice, Rice-Rapeseed-Rice, Jute-Rice-Rice, Jute-Pulses-Rice (Biswas *et al*., 2006).

Several researchers (Moratiel *et al*., 2011; *Huo et al*., 2013; Delghandi *et al*., 2017; Gimenez and Garcia-Galiano, 2018; Dong *et al*., 2019a; Yang *et al*., 2020; Ouhamdouch *et al*., 2020) have used General Circulation Models (GCMs) or Regional Climatic Models (RCMs) to find relationship between evapotranspiration and climate change. In a more recent trend analysis study conducted by Ndiaye *et al*. (2021) in Senegal River Basin, West Africa, a significant increment was seen in PET from 2036-2065. Theoretically, global warming would increase evapotranspiration, but some regions disagreed with this inference. Hobins *et al*. 2004 researched on trend analysis of actual ET and pan evaporation across U.S. and documented results showing a decrease in PET over time. Roderick and Farquehar (2002) also made similar conclusions. Research done in Canada (Burn and Hesch, 2007), Greece (Papaioannou *et al*. 2007), India (Chattopadhyay and Hulme, 1997), Thailand (Tebakari *et al*. 2005) and Japan (Asanuma and Kamimera, 2004) showed likewise. However, these researches were conducted in the past decades and are unlikely to reflect on modern climatic environment. Banerjee and Biswas (2020) assessed that the impact of climate change on future evapotranspiration in West Bengal (India), which showed an increment of 13-32% in RET by 2050 along with reducing trend in post-autumnal showers.

In addition, large-scale water fluxes are determined by climatic factors (Yuan and Bai, 2018; Chen *et al*., 2012). The response of evapotranspiration rates is diverse and shows regional variations [Shi *et al*., 2013]. Therefore, understanding how climate change affects hydrology of a particular region is imperative.

General Circulation Models (GCMs) do not find any direct use for regional hydrological models (Wigley *et al*., 1990; Carter *et al*., 1994). Statistical downscaling helps in providing a relation between global and local variables. Systematic relationship is utilized by statistical downscaling techniques from the observed data (Wigley *et al*., 1990). MarkSim Weather generator is one such efficient tool to downscale data, particularly in this case, as it requires minimal data input and has global data applicability (Trotochaud *et al*., 2016).

Estimation of PET can be made via several methods. Research has demonstrated that the PET formula employed determines how climate change affects discharge (Seiller and Anctil, 2016; Bae *et al*., 2011; Sperna Weiland *et al*., 2012). According to 2013 IPCC Report, anthropogenic CO_2 emissions will continue to have major influence on global temperatures throughout the course of the next century, and as a result, the estimated PET increases significantly when temperature-based calculations are used. To provide evidence of the effect of global warming on future PET and crop water requirements, estimation of PET has been carried out primarily with two temperature based empirical approaches- Hargreaves-Samani (H/S) method (Hargreaves and Samani, 1985; Samani, 2000) and Turc method (Turc, 1961) and to support them Makkink method (Makkink, 1957) has been used. Relation between ET and rainfall has been made to assess their combined impact on future water requirement availability to improve management strategies. In the past years, particularly last decade, many research studies, have been carried out worldwide, aiming the hydrological projections of evapotranspiration and rainfall using empirical methods. However, in India, very few studies focused on a regional scale targeting future ET and rainfall pattern, especially on a long – term basis and how it might affect the future of

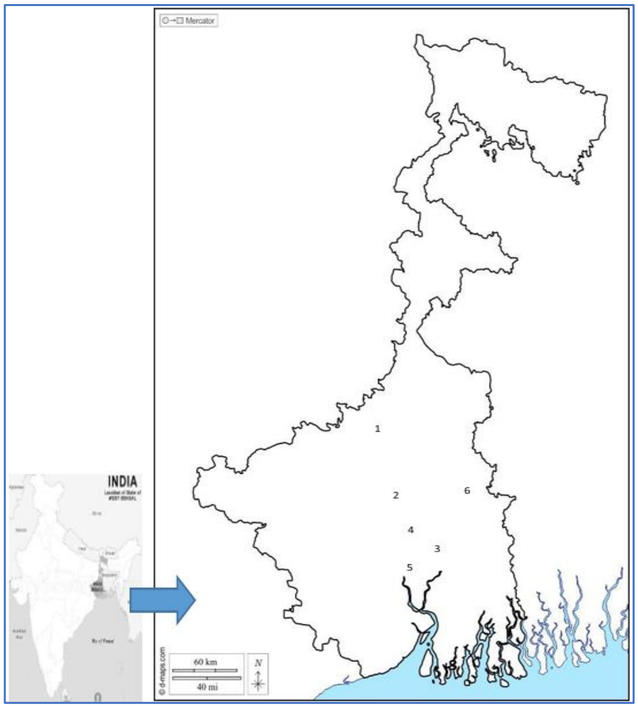

Fig. 1. Map of West Bengal showing study locations (1: Bolpur, Red laterite zone; 2: Burdwan, Old alluvial zone; 3: Canning, Coastal and saline zone; 4: Hooghly, New alluvial zone; 5: Howrah, New alluvial zone; 6: Kalyani, New alluvial zone)

irrigation and crop growth. No published study has ever projected future ET in the LGP region of India. The paucity of studies, in this specific region, has motivated us to conduct the study. It analyses the variability of ET and rainfall taking into account temperature (minimum and maximum) and solar radiation for hydrological forecasts for the 21st century using two Representative Concentration Pathways (RCP) scenarios: an uncontrolled climate change scenario with continuous high greenhouse gas emissions (RCP8.5) and a midway greenhouse gas mitigation scenario (RCP4.5). Empirical methods have been used to find daily PET estimates for six stations using three GCMs namely, GFDL-ESM2G, HadGEM2-ES and MIROC5 under RCP 4.5 and 8.5 scenarios for the future. Daily values were then summed up and averaged for the time period to find monthly total value for each method used to project the future PET pattern. The differences in PET estimates as indicated by future projections and baseline period have been studied to understand the climate change impact on PET process under both RCPs, separately.

Therefore, the major objectives of performing the study were: 1) to assess the outcomes of H/S, Turc and Makkink methods in relation to FAO PM method, 2) to observe the variation of future PET and effective rainfall for projected climatic scenario of RCP 4.5 and 8.5, 3) to assess the trend of the difference between effective rainfall and PET for both scenarios.

2. Study area

The Lower Gangetic Plains region forms a sub-division of the Indo-Gangetic Plain. It is one of the fifteen agroclimatic zones in India spanning an area of approximately 81,000 km² (Sirohi, 1989). This region specifically falls under the state of West Bengal. Agriculture plays an important role in the economy, providing livelihood for 70% people of this region. Rice and potato are the main cultivated crops. Alternate periods of flood and drought make growing of crops quite unpredictable. The average rainfall is 157 cm annually. Ground water utilization of this region is more than 35%. However, changing and warming climate has threatened the farming practice here due to augmented water scarcity despite of plentiful precipitation.

Six stations of LGP viz., Bolpur, Burdwan, Canning, Hooghly, Howrah and Kalyani, with climatic diversity, have been considered for this study [Fig. 1]. The zone, in general, shows tropical climate with hot summers and moderately cold winters. The day temperature during summer months ranges from 38 °C to 45 °C while the winter temperature may fall to 6 °C to 7 °C. Monsoons start in the month of June caused solely due to the current of winds developed in the Bay of Bengal. The annual precipitation lies between 140 cm - 170cm approximately [Table 1].

3. Simulated Data collection

The present study is based on secondary data of climatic parameters simulated for the future, in two time slices (2030-2050) and (2070-2090) along with baseline (2010-2020), derived from MarkSim GCM - DSSAT Weather File Generator - the online version for IPCC CMIP5 data (MarkSim® GCM - DSSAT weather file generator (cgiar.org)). Temperature (minimum and maximum) and global solar radiation (GSR) have been simulated along with rainfall for six stations. Statistical downscaling is done which uses the output of the GCM to compute a statistical relationship with existing meteorological data from observatory which is then used to scale the results of the GCM to that of the station of the particular location. To create long-term weather data for crop production simulations, MarkSim is a frequently used weather generator (*e.g.*, Mavromatis and Hansen, 2001; Jones and Thornton, 2003; Thornton *et al*., 2009; Claessens *et al*., 2012; Jones and Thornton, 2013). MarkSim has been used over other methods as it has minimal input requirements and global database applicability (Trotochaud *et al*., 2016).

TABLE 1

Geographic coordinates, altitude, soil type and annual rainfall of the six stations on which the study was done

Location	ID as in Fig 1.	LAT (ºN)	LONG (ºE)	Altitude (Above m. s. l.) (m)	Soil type	Annual rainfall (mm)
Bolpur	1	23º40`	87º43`	58	Red lateritic	1476
Burdwan	2	23º13`	87º51`	40	Coarse sandy	1496
Canning	3	22º31`	88º66`	6	Fine loamy	1746
Hooghly	4	22º90`	88º39`	200	Clay sandy loam	1500
Howrah	5	22º57`	88º32`	7	Clay loam	1744
Kalyani	6	22º97`	88º43`	14	Silty clay	1467

TABLE 2

Brief of the GCMs used in this study

Model	Institution	Resolution (Lat × Long i)	Reference
GFDL-ESM2G	Geophysical Fluid Dynamics Laboratory	2..0 x 2.5	Dunne *et al*. (2012).
HadGEM2-ES	Met Office Hadley Centre	1.2414 x 1.875	Collins *et al*. (2011). .
MIROC5	Japan Agency for Marine- Earth Science and Technology, Atmosphere and Ocean Research Institute (The University of Tokyo), and National Institute for Environmental Studies	1.4063 x 1.4063	Watanabe *et al*. (2010).

(*source*: *MarkSim*™ *GCM* - *DSSAT* weather file generator - Documentation)

In this study, multi-model bi-scenario projection has been made by taking the average (ENSEMBLE) of three GCM models - GFDL-ESM2G, HadGEM2-ES, and MIROC5 (details of which are given in Table 2) and RCPs 4.5 and 8.5 scenarios. Although, the multi-model ensemble (MME) provides a more realistic representation of the climate system as compared to individual models (Taylor *et al*., 2012; Yin *et al*., 2015; Dong et al., 2019b), MME from all 17 models would have reduced interannual variability and therefore lower the range of water availability, affecting its projection.

The said models have been chosen from a pool of 17 models (available in MarkSimGCM) based on performance evaluations by multiple researchers such as Srinivasa Raju & Nagesh Kumar, 2015; Srinivasa Raju, Sonali & Nagesh Kumar, 2017; Chandran *et al*., 2022.

3.1. *Weather data collection from observatory*

Climatic data for the baseline period (2010-2020) was collected from the observations made by the meteorological observatory maintained by All India Coordinated Research Project on Agrometeorology (AICRPAM) compared with those obtained from MarkSim Weather Generator to see to what extent model run data matches with actual data.

3.2. *Evaluation of PET*

To evaluate PET for present weather situation and future climatic scenario, H/S method (Hargreaves and Samani, 1985; Samani, 2000) (eqn.1), Turc Method (Turc, 1961) (eqn. 2) and Makkink Method (Makkink, 1967) (eqn. 3) were used. The former two are temperature - based while the latter is a radiation based empirical model. While there are certain drawbacks with the temperature-based PET formula compared to the physically based formula, the latter is not a readily available formula because it requires a large number of meteorological variables and observational data. However, when evaluating PET from in-situ observed data, FAO Penman Method (eqn. 4) (Allen *et al*., 1998) was used which is considered one of the best methods to measure PET with maximum accuracy, as stated by various past researchers and authors (Debnath *et al*., 2015; Sentelhas *et al*., 2010). Depending available data, formulae used for calculation of PET with the aforementioned methods have been shown in eqns. 1, 2, 3 and 4.

$$PET = 0.0023\,(\bar{T} + 17.8) * \sqrt{(T_{max} - T_{min})} * Ra \quad (1)$$

$$PET = 0.013 * 23.88 * [\bar{T}/(\bar{T}+15)] * (R_s + 50) \quad (2)$$

$$PET = 0.61 * [\Delta / (\Delta+0.0665)] * (R_s / 2.45) – 0.12 \quad (3)$$

$$PET = \frac{0.408\,\Delta\,(R_n - G) + \gamma \frac{900}{T+273} u_2\,(e_s - e_a)}{\Delta + \gamma\,(1 + 0.34\,u_2)} \quad (4)$$

where, the potential evapotranspiration [mm/day] is represented by PET; T_{max} is the daily highest temperature [°C] and $\bar{T}$ is the daily mean temperature [°C]. Daily minimum temperature [°C] is denoted by T_{min}. [MJ/m^2/day] is the extra terrestrial radiation, or R_a. R_s stands for solar radiation or incident solar radiation [MJ/m²/day]. The slope vapor curve (Δ) is expressed in kPa °C^{-1}, the crop surface net radiation (R_n) is expressed in MJm^{-2}day^{-1}, and the soil heat flux density (G) is expressed in MJm^{-2}day^{-1}. The e_s is the saturation vapor pressure (kPa); e_a is the actual vapor pressure (kPa); T is the air temperature at 2 m height (°C);

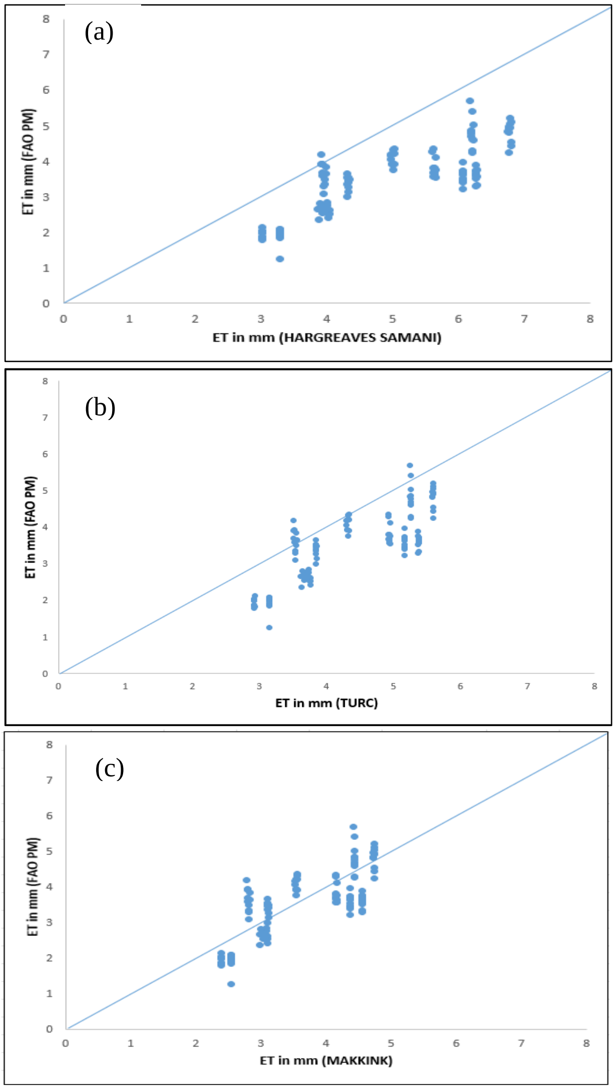

Figs. 2(a-c). The 1:1 line between daily PET values as estimated by (a) HS, (b) Turc and (c) Makkink methods against the FAO PM method

u_2 is the wind speed at 2 m height (m/s); where γ (kPa °C^{-1}) is the psychrometric constant.

To measure the accuracy and reliability of PET methods used in this study, monthly total PET estimates by each method of the study region were compared with those estimated by FAO PM method and their performances were evaluated. Error in PET estimates from alternate methods were quantified in relation to FAO Penman using (1) Mean Bias Error (MBE), which gave an overall average of the error stating whether PET was under or over-estimated by considering sign of the error; (2) root mean square error, that showcases how concentrated the PET was around the line of best fit; (3) percent BIAS (PBIAS) which quantified the average tendency of the model to overpredict or underpredict observed values; and their relationship was studied using Pearson correlation coefficients which gave a measure of association between the PET estimates.

3.3. *Calculation of Effective rainfall*

There are quite a few methods for calculating effective rainfall like Renfro Equation, U.S. Bureau of Reclamation method, Potential evapotranspiration / precipitation ratio method (India), U.S.D.A. Soil Conservation Service (SCS) method and empirical relationships. Here, U.S.D.A. SCS method for calculating effective rainfall (Obreza and Pitts, 2002) has been used for both observed and predicted data. However, it is frequently seen that temperature can be more accurately simulated using GCM data than precipitation, especially when it comes to regional distributions (Yuan and Bai, 2018). The U.S.D.A. created this technique after analyzing long-term soil moisture and climate data. 22 experimental stations with fifty years' worth of precipitation data that represented various meteorological and soil conditions were analyzed. This method was developed keeping in mind that the monthly E.R. always be less than plants' consumptive use. This method has medium accuracy and low relative costs. The formula (eqn. 5) used in calculation effective rainfall is as-

$$E.R. = (P * (125 - 0.2 * 3 * P)) / 125; \text{ for } P <= 250 / 3 \text{ mm} \quad E.R. = 125 / 3 + 0.1 * P; \text{ for } P > 250 / 3 \text{ mm} \qquad (5)$$

It must be noted that with high precipitation, the precipitation water loss is also high.

4. Results

Performance of Hargreaves-Samani (HS), Turc and Makkink method in relation to FAO 56 Penman Monteith (PM) method

The PET values calculated through HS, Turc and Makkink nethods for all the stations for past 11 years were compared with FAO56 PM method. Table 3 shows the error and correlation values of the three PET methods used in the study against the PM method. The correlation coefficients for all the methods were very close to each other. The MBE and RMSE was found to be lowest in Makkink method and highest for Hargreaves-Samani method. Small value of RMSE and MBE indicates lower disagreement between FAO PM and the empirical method under consideration. The best model was selected based on their orientation along the 1:1 line graph [Fig. 2], the lowest value of MBE, RMSE and PBIAS and a strong correlation coefficient. The HS method chiefly overestimated the PET values [Fig. 2a]. The factor responsible for such overestimation by HS could be the high difference between maximum and minimum temperature (T_{max} - T_{min}) which

TABLE 3

Error structure and correlation between the estimated PET derived by Hargreaves-Samani, Turc and Makkink methods and FAO Penman Monteith method

PET Methods	Mean Bias Error (MBE)	Root Mean Square Error (RMSE)	Pearson's correlation coefficient	Percent BIAS (PBIAS)
Hargreaves-Samani vs FAO Penman Monteith	1.3	1.6	0.84	42.45
Turc vs FAO Penman Monteith	0.84	1.01	0.83	25.49
Makkink vs FAO Penman Monteith	0.12	0.56	0.82	4.17

forms an essential component in the HS equation. The MBE, RMSE and PBIAS values were considerably low (0.12, 0.56 and 4.17 respectively) for the Makkink method [Table 3]. Deflections of PET values from 1:1 line have also been observed in Turc method [Fig 2b]. But in case of Makkink method the PET data are well oriented along with 1:1 line [Fig 2c]. Thus, considering the cumulative performance for 11 years (2010-2020), it was ascertained that the Makkink method could efficiently reconstruct the ET pattern with simulated input data with least error and deviation and therefore, in this paper, the Makkink method has been given priority in predicting actual ET for post-monsoon and pre-monsoon seasons under climate change scenario.

The mean increase in temperature (represented by $\overline{T}$) over the century was alike for all the stations. Increment in daily $\overline{T}$ roughly ranged from 1.76 ℃ (as seen in Canning) to 1.9 ℃ (as in Bolpur) for RCP 4.5 over the said time frame; whereas temperature ($\overline{T}$) is projected to rise by 3.96 ℃ in Canning and 4.22 ℃ in Kalyani for RCP 8.5 scenario. Highest temperature is likely to be recorded at Bolpur (RCP 4.5) and Kalyani (RCP 8.5). The variation of $\overline{T}$ for the months of March, April, May (pre-monsoon) [Table 4A and 4B] and October, November and December (post-monsoon) [Table 5A and 5B] are shown for the periods 2030-2050 (mid-century) and 2070-2090 (late-century) under both scenarios, respectively.

For pre-monsoon period, it is observed that during the mid-century, projected $\overline{T}$ ranges from 31 ℃ to 32.6 ℃ for RCP 4.5 whilst for RCP 8.5, it varies from 30.98 ℃ to 32.8 ℃ [Table 4A]. The range of projected $\overline{T}$ for end-century varies from 32.13 ℃ to 33.7 ℃ (RCP 4.5) and 33.14 ℃ to 35.5 ℃ (RCP 8.5) [Table 4B].

For post-monsoon period, it is observed that during the mid-century, projected $\overline{T}$ ranges from 26.07 ℃ to 27.45 ℃ for RCP 4.5 whilst for RCP 8.5, it varies from 26.14 ℃ To 27.88 ℃ [Table 5A]. The range of projected $\overline{T}$ for end-century varies from 27.06 ℃ to 28.21 ℃ (RCP 4.5) and 28.48 ℃ to 30.75 ℃ (RCP 8.5) [Table 5B].

4.1. *Rainfall projection under changed climatic scenario*

The future precipitation pattern is decisive in giving an idea on drought assessment adaption and mitigation techniques to overcome it. Although its significance is not as pivotal in humid and sub-humid regions (area under study) as in dry and semi- arid areas, a brief knowledge of the same can prove handy in predicting soil moisture status and understanding crop water requirement, especially in irrigation-based locations.

Rainfall has been projected differently under the two different climatic scenarios. Rainfall in the six stations under study was mainly towards the high end; however, few anomalies could be seen. Regarding rainfall, no uniform trend was observed for the various time slices considered. June and July were the months of highest rainfall. It is the time of onset of South West monsoon. November and December received little to no rainfall on isolated days throughout the century. October witnessed high precipitation (due to the collision between retreating South West monsoon wind and incoming North East wind which caused cyclonic depression). Pre-monsoon showers occurred in the months of March and April. January received light showers which decreased by February. Overall, Howrah experienced maximum precipitation and Burdwan received the least rain [Fig. 3(a) and 3(b)].

4.2. *Rainfall under RCP 4.5 scenario*

In Howrah, highest rainfall was recorded during the baseline period (610 mm in June) [Fig. 3(a)]. Rainfall decreased in the mid-century but increased perpetually in the late century time slice in Kalyani, Canning and Howrah. No rain in December and negligible rainfall in November was a common trait for all areas under study. Fig. 3(a) shows variation of present and future rainfall (under RCP 4.5 scenario) of the six stations under study. Increasing trend of rainfall was projected for Hooghly and Canning stations. Burdwan (mid-century) and Hooghly was anticipated to receive considerable rain in September and very restricted rain in October (a deviation from general trend followed in all stations). Studies by different authors using CMIP5 models have highlight a rise in seasonal precipitation, driven by enhanced monsoonal activity due to increased atmospheric moisture content (Das *et al*., 2020; Mallik and Ghosh, 2022).

TABLE 4A

Projected daily average temperature during the pre-monsoon period for 2030-2050 (mid-century)

Year	BOLPUR		BURDWAN		CANNING		HOOGHLY		HOWRAH		KALYANI	
	RCP 4.5	**RCP 8.5**	**RCP 4.5**	**RCP 8.5**	**RCP 4.5**	**RCP 8.5**	**RCP 4.5**	**RCP 8.5**	**RCP 4.5**	**RCP 8.5**	**RCP 4.5**	**RCP 8.5**
2030	31.6	31.62	31.33	31.82	31	30.89	31.45	31.47	31.34	31.25	31.3	31.42
2031	31.63	31.66	31.38	31.86	31.05	30.98	31.52	31.52	31.39	31.33	31.35	31.46
2032	31.68	31.71	31.44	31.9	31.09	31.04	31.56	31.56	31.43	31.38	31.39	31.52
2033	31.73	31.77	31.44	31.95	31.13	31.09	31.6	31.62	31.47	31.43	31.43	31.57
2034	31.77	31.82	31.49	31.96	31.17	31.14	31.65	31.68	31.51	31.48	31.47	31.63
2035	31.81	31.88	31.55	32.01	31.21	31.19	31.7	31.73	31.55	31.54	31.52	31.68
2036	31.85	31.94	31.6	32.05	31.25	31.24	31.74	31.79	31.59	31.59	31.55	31.73
2037	31.9	32	31.66	32.09	31.25	31.3	31.79	31.85	31.63	31.64	31.59	31.8
2038	31.93	32.05	31.72	32.13	31.33	31.35	31.83	31.9	31.67	31.7	31.64	31.85
2039	31.98	32.05	31.87	32.17	31.36	31.4	31.87	31.96	31.71	31.75	31.67	31.91
2040	32.02	32.17	31.93	32.21	31.4	31.46	31.91	32.02	31.74	31.81	31.7	31.97
2041	32.05	32.23	31.99	32.24	31.43	31.51	32.05	32.08	31.78	31.86	31.74	32.03
2042	32.09	32.29	32.04	32.28	31.46	31.57	32.07	32.14	31.81	31.92	31.78	32.07
2043	32.29	32.35	32.1	32.39	31.5	31.62	32.11	32.19	31.85	31.98	31.82	32.13
2044	32.25	32.41	32.16	32.42	31.54	31.68	32.14	32.25	31.88	32.03	31.85	32.19
2045	32.28	32.47	32.22	32.46	31.57	31.73	32.17	32.31	31.92	32.09	31.88	32.25
2046	32.32	32.47	32.28	32.49	31.6	31.79	32.21	32.37	31.95	32.15	31.91	32.31
2047	32.35	32.58	32.34	32.52	31.63	31.85	32.25	32.43	31.98	32.21	31.95	32.37
2048	32.39	32.65	32.4	32.56	31.66	31.9	32.28	32.49	32.01	32.26	31.98	32.43
2049	32.41	32.71	32.46	32.59	31.69	31.96	32.31	32.54	32.04	32.33	32.01	32.5
2050	32.45	32.77	32.52	32.62	31.72	32.02	32.34	32.61	32.08	32.38	32.04	32.56

TABLE 4B

Projected daily average temperature during the pre-monsoon period for 2070-2090 (end-century)

Year	BOLPUR		BURDWAN		CANNING		HOOGHLY		HOWRAH		KALYANI	
	RCP 4.5	**RCP 8.5**	**RCP 4.5**	**RCP 8.5**	**RCP 4.5**	**RCP 8.5**	**RCP 4.5**	**RCP 8.5**	**RCP 4.5**	**RCP 8.5**	**RCP 4.5**	**RCP 8.5**
2070	32.98	34.11	33.12	33.78	32.14	33.09	32.78	33.85	32.52	33.61	32.49	33.79
2071	33	34.15	33.14	33.82	32.16	33.14	32.8	33.91	32.54	33.66	32.51	33.9
2072	33.02	34.18	33.17	33.9	32.17	33.2	32.81	33.98	32.56	33.72	32.52	33.97
2073	33.05	34.28	33.19	33.97	32.18	33.27	32.83	34.05	32.58	33.79	32.54	34.03
2074	33.07	34.35	33.21	34.04	32.2	33.33	32.84	34.12	32.6	33.85	32.55	34.1
2075	33.17	34.42	33.23	34.11	32.22	33.4	32.86	34.18	32.61	33.92	32.57	34.17
2076	33.19	34.49	33.25	34.18	32.23	33.46	32.88	34.25	32.63	33.98	32.59	34.24
2077	33.21	34.56	33.28	34.25	32.25	33.52	32.9	34.32	32.65	34.05	32.61	34.3
2078	33.23	34.63	33.34	34.32	32.26	33.59	32.92	34.39	32.67	34.11	32.63	34.38
2079	33.26	34.7	33.37	34.39	32.28	33.65	32.93	34.46	32.69	34.18	32.65	34.45
2080	33.28	34.78	33.39	34.42	32.3	33.72	32.95	34.53	32.71	34.25	32.67	34.52
2081	33.23	34.87	33.42	34.46	32.32	33.79	32.97	34.6	32.72	34.32	32.69	34.59
2082	33.26	34.94	33.45	34.6	32.33	33.85	33	34.67	32.75	34.38	32.71	34.66
2083	33.29	35.01	33.47	34.59	32.35	33.92	33.02	34.66	32.77	34.45	32.73	34.73
2084	33.32	35.09	33.5	34.66	32.37	33.98	33.04	34.73	32.79	34.52	32.75	34.81
2085	33.35	35.17	33.53	34.74	32.39	34.06	33.07	34.8	32.82	34.59	32.77	34.88
2086	33.38	35.25	33.55	34.81	32.41	34.06	33.11	34.88	32.84	34.66	32.8	34.95
2087	33.42	35.33	33.58	34.89	32.44	34.19	33.03	34.97	32.86	34.67	32.83	35.03
2088	33.45	35.4	33.61	34.96	32.46	34.17	33.06	35.04	32.89	34.74	32.85	35.11
2089	33.49	35.48	33.65	35.05	32.48	34.24	33.09	35.12	32.91	34.82	32.88	35.18
2090	33.56	35.56	33.68	35.12	32.51	34.31	33.13	35.19	32.94	34.89	32.9	35.26

TABLE 5A

Projected daily average temperature during the post-monsoon period for 2030-2050 (mid-century)

Year	BOLPUR		BURDWAN		CANNING		HOOGHLY		HOWRAH		KALYANI	
	RCP 4.5	**RCP 8.5**	**RCP 4.5**	**RCP 8.5**	**RCP 4.5**	**RCP 8.5**	**RCP 4.5**	**RCP 8.5**	**RCP 4.5**	**RCP 8.5**	**RCP 4.5**	**RCP 8.5**
2030	26.03	26.11	26.08	26.64	26.73	26.84	26.48	26.57	26.43	26.76	26.40	26.68
2031	26.07	26.14	26.12	26.69	26.77	26.90	26.52	26.62	26.47	26.80	26.44	26.71
2032	26.12	26.19	26.16	26.74	26.78	26.95	26.56	26.67	26.51	26.85	26.48	26.78
2033	26.16	26.24	26.20	26.74	26.82	27.00	26.61	26.72	26.55	26.90	26.52	26.83
2034	26.20	26.30	26.05	26.80	26.87	27.05	26.66	26.78	26.59	26.96	26.56	26.84
2035	26.25	26.35	26.28	26.85	26.89	27.10	26.70	26.83	26.64	27.00	26.61	26.89
2036	26.29	26.41	26.33	26.95	26.93	27.15	26.75	26.89	26.67	27.06	26.64	26.94
2037	26.33	26.46	26.37	27.01	26.93	27.20	26.79	26.93	26.71	27.10	26.68	27.00
2038	26.38	26.52	26.41	27.05	27.01	27.25	26.83	27.07	26.75	27.15	26.72	27.06
2039	26.41	26.52	26.44	26.93	27.05	27.30	26.87	27.13	26.79	27.21	26.76	27.11
2040	26.45	26.63	26.49	26.98	27.09	27.35	26.73	27.18	26.83	27.21	26.80	27.17
2041	26.50	26.69	26.52	27.03	27.12	27.41	26.77	27.23	26.86	27.31	26.84	27.22
2042	26.53	26.74	26.57	27.09	27.16	27.46	26.87	27.29	26.90	27.37	26.87	27.35
2043	26.21	26.79	26.40	27.14	27.20	27.51	26.91	27.34	26.94	27.42	26.90	27.40
2044	26.42	26.84	26.45	27.20	27.23	27.56	26.95	27.39	26.97	27.47	26.95	27.46
2045	26.47	26.90	26.48	27.25	27.26	27.62	26.98	27.45	27.01	27.53	26.98	27.51
2046	26.50	26.90	26.52	27.31	27.29	27.66	27.02	27.50	27.04	27.58	27.01	27.57
2047	26.54	27.02	26.56	27.37	27.33	27.72	27.05	27.52	27.08	27.63	27.05	27.63
2048	26.57	27.08	26.59	27.42	27.39	27.77	27.08	27.61	27.11	27.69	27.08	27.68
2049	26.61	27.13	26.62	27.51	27.43	27.83	27.12	27.63	27.15	27.74	27.12	27.74
2050	26.38	27.20	26.65	27.57	27.45	27.88	27.13	27.73	27.18	27.80	27.15	27.79

TABLE 5B

Projected daily average temperature during the post-monsoon period for 2070-2090 (end-century)

Year	BOLPUR		BURDWAN		CANNING		HOOGHLY		HOWRAH		KALYANI	
	RCP 4.5	**RCP 8.5**	**RCP 4.5**	**RCP 8.5**	**RCP 4.5**	**RCP 8.5**	**RCP 4.5**	**RCP 8.5**	**RCP 4.5**	**RCP 8.5**	**RCP 4.5**	**RCP 8.5**
2070	27.07	28.45	27.2	28.78	27.93	29.23	27.62	28.95	27.69	29.11	27.66	29.01
2071	27.09	28.49	27.21	28.84	27.94	29.28	27.64	28.98	27.72	29.05	27.68	29.05
2072	27.1	28.54	27.24	28.93	27.96	29.35	27.65	29.04	27.73	29.11	27.7	29.12
2073	27.12	28.64	27.25	28.96	27.98	29.41	27.67	29.11	27.75	29.18	27.72	29.19
2074	27.14	28.71	27.28	29.03	27.99	29.47	27.69	29.19	27.77	29.24	27.74	29.27
2075	27	28.79	27.3	29.1	28.01	29.53	27.7	29.25	27.78	29.32	27.75	29.33
2076	27.02	28.86	27.32	29.18	28.02	29.6	27.72	29.33	27.8	29.38	27.77	29.41
2077	26.98	28.94	27.33	29.26	28.03	29.67	27.74	29.41	27.82	29.45	27.79	29.48
2078	27	29.02	27.35	29.33	28.05	29.74	27.75	29.47	27.84	29.52	27.8	29.56
2079	27.01	29.1	27.37	29.41	28.06	29.82	27.78	29.55	27.86	29.6	27.82	29.64
2080	27.03	29.18	27.39	29.45	28.08	29.89	27.79	29.63	27.86	29.69	27.84	29.71
2081	27.22	29.26	27.41	29.49	28.1	29.96	27.81	29.7	27.88	29.76	27.85	29.79
2082	27.24	29.35	27.43	29.65	28.11	30.03	27.82	29.78	27.89	29.84	27.86	29.87
2083	27.25	29.43	27.45	29.9	28.12	30.11	27.84	30.04	27.9	29.91	27.88	29.95
2084	27.27	29.52	27.47	29.98	28.13	30.18	27.85	30.13	27.94	30	27.89	30.03
2085	27.29	29.6	27.48	30.07	28.14	30.25	27.87	30.2	27.96	30.07	27.91	30.11
2086	27.31	29.7	27.5	30.21	28.15	30.25	27.79	30.28	27.97	30.15	27.92	30.2
2087	27.33	29.77	27.52	30.29	28.17	30.4	27.99	30.36	27.95	30.38	27.92	30.29
2088	27.35	29.86	27.54	30.38	28.18	30.6	28	30.45	27.97	30.47	27.94	30.38
2089	27.37	29.95	27.56	30.47	28.19	30.68	28.02	30.54	27.98	30.55	27.95	30.47
2090	27.39	30.05	27.59	30.55	28.21	30.76	28.04	30.63	28	30.61	27.96	30.57

Fig. 3(a) Variation of present and future rainfall (under RCP 4.5 scenario) of six stations under study

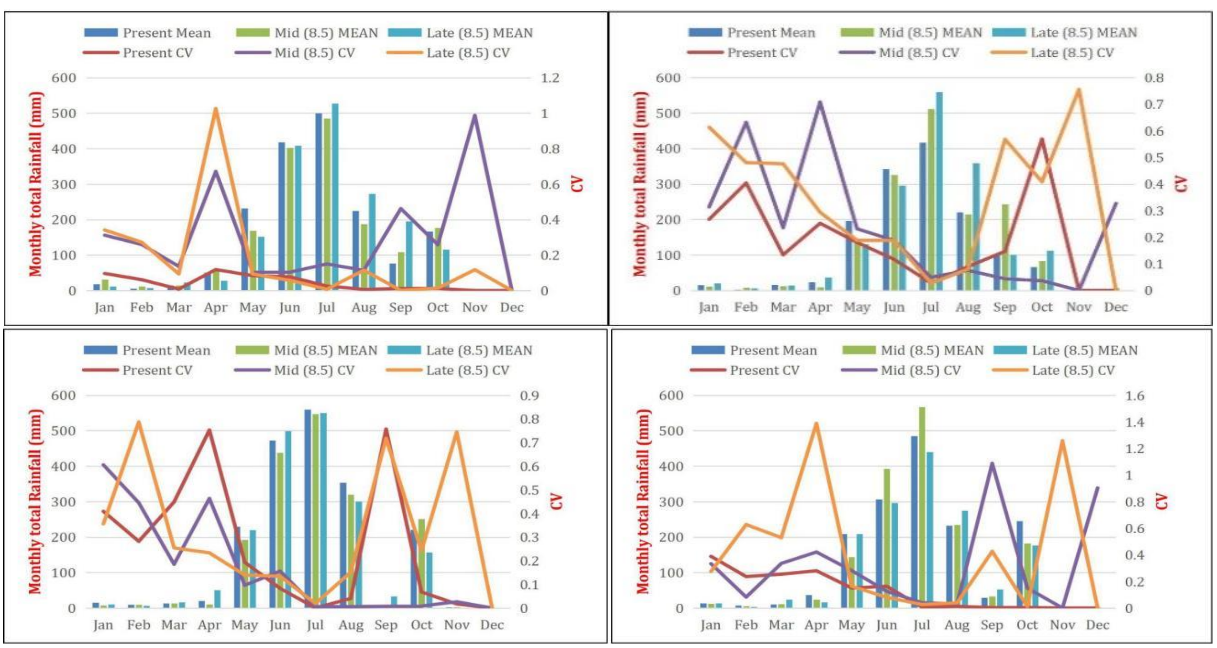

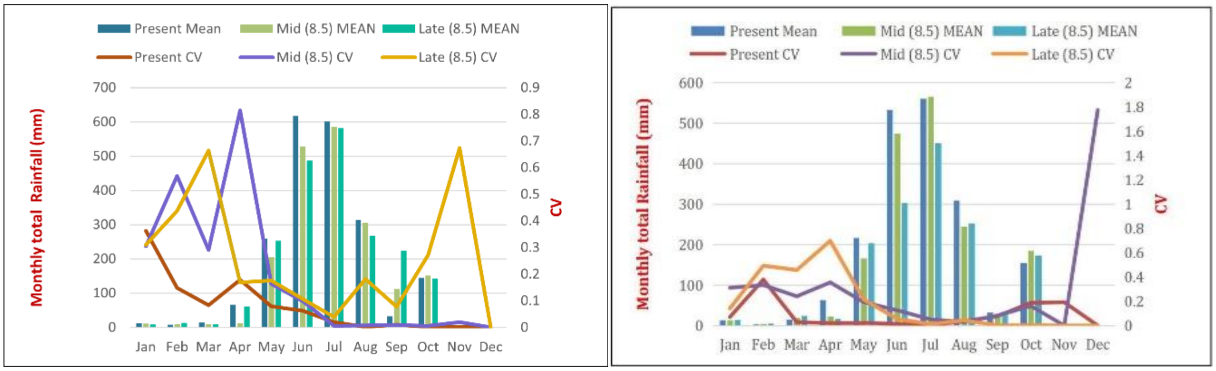

Fig. 3(b). Variation of present and future rainfall (under RCP 8.5 scenario) of six stations under study

4.3. *Rainfall under RCP 8.5 scenario*

Fig. 3(b) shows variation of present and future rainfall (under RCP 8.5 scenario) of the six stations under study. The amount of precipitation was higher than the RCP 4.5 scenario in case of Howrah and Burdwan stations [when comparing both Figs. 3(a&b)]. Kalyani received comparatively low rainfall, declining gradually by the century. Such diminishing trend was also seen for Hooghly, Canning and Bolpur (mid-century) stations. No rainfall in November and isolated rain in December (2045-2050) [as evident from the graph Fig. 3(b)], usually between the 10th and 12th day of the month for Kalyani was expected. In Bolpur, some rain in November could be seen. The results showed that changes in predicted rainfall in most cases were within an acceptable range (Debnath *et al*., 2023).

4.4. *Variation of PET under projected climatic scenario for RCP 4.5 and 8.5*

PET is expected to rise globally and regionally due to higher temperatures and increased vapor pressure deficits. For instance, studies project a 4–8% increase in annual PET by 2040-2059 compared to historical periods under RCP 8.5 scenarios (Shamir *et al*., 2024). All three methods showed a rise in PET (Table 6 and 7). In general, PET increment from mid-century to late century is higher than from baseline to mid-century except in Bolpur where the difference is higher from baseline to mid and in Burdwan where the increment was uniform throughout. Maximum PET growth over the century has been observed in Howrah. In some areas of West Bengal, particularly the southern region, PET increases could reach up to 31.8% by 2050 compared to baseline levels (Banerjee and Biswas, 2020).

If we consider the annual scale variation, it is observed that the ensemble mean PET for LGP is expected to increase at ~2 mm/year (mid- century) and ~ 1 mm/year (late - century) under RCP 4.5. Pre-monsoon months experience more pronounced PET changes coinciding with higher temperatures; RCP 8.5 being the higher emission scenario shows the greatest rise [evident from tables 6 and 7] Similar results have been found by researchers who predicted future PET using CMIP5 models. Very high PET values were projected for Howrah and Kalyani in the month of May under both scenarios.

Inclination of the monthly dataset is similar to those of the daily. Table 6 and 7 shows monthly variation in PET for different stations under study. January was the month with lowest PET estimate while May showed the highest value. Mean monthly PET values varied from 93.5 mm in January to 208.2 mm in May. Kalyani and Howrah stations showed maximum variation between winter and summer PET values. A steady fall in PET was seen after May which continues decreasing further after a slight increase in August. Burdwan was the only station where the mean monthly PET values had been found highest in April (also seen during baseline period). The simulation projects an overall increase in PET in all the stations in the mid-century timeline. The significant contribution of monthly PET to annual PET in order of rank, was highest in the month of May (except in Burdwan) followed by April, June and March. Towards the end century, the orientation in PET rates showed slight variation. The rate of increase of PET estimates were expected to slim down and in certain months like January, October and November PET estimates were projected to decrease towards the late century period. This was an aberration from the principal relation between temperature and ET variation which stated that with an increase in temperature, PET was likely to increase.

Intra-annual variability was lower compared to other data sets. The ensemble mean PET for LGP is expected to increase at ~2.5 mm/year (mid - century) and ~3.9 mm/year (late century) under RCP 8.5. The increase/decrease in daily PET was not uniform in all the six stations. Howrah showcased the highest PET value by the end of century.

TABLE 6

Variation of present and future PET as calculated through Makkink's method (RCP 4.5) for different study location

Month	BOLPUR			BURDWAN			CANNING		
	Present	Future mid	Future late	Present	Future mid	Future late	Present	Future mid	Future late
Jan	64.72 (0.026)	70.63 (0.045)	72.86 (0.007)	70.05 (0.004)	68.8 (0.012)	72.97 (0.008)	74.69 (0.012)	76.11 (0.007)	80.09 (0.003)
Feb	82.08 (0.004)	84.34 (0.119)	82.34 (0.008)	80.07 (0.004)	80.90 (0.019)	80.55 (0.011)	86.38 (0.003)	89.30 (0.01)	92.66 (0.002)
Mar	124.94 (0.002)	126.91 (0.012)	126.5 (0.004)	120.42 (0.012)	127.52 (0.014)	133.96 (0.007)	126.49 (0.002)	129.03 (0.006)	132.12 (0.0013)
April	131.89 (0.005)	133.03 (0.004)	133.79 (0.005)	133.58 (0.002)	131.86 (0.002)	134.44 (0.008)	132.95 (0.001)	134.65 (0.004)	137.14 (0.0009)
May	133.41 (0.0049)	133.48 (0.028)	135.3 (0.005)	123.36 (0.019)	126.24 (0.015)	119.21 (0.006)	142.10 (0.001)	143.90 (0.004)	146.71 (0.002)
Jun	113.83 (0.052)	118.92 (0.054)	111.51 (0.045)	114.63 (0.039)	118.36 (0.009)	111.12 (0.014)	100.92 (0.003)	104.1 (0.009)	107.13 (0.008)
Jul	91.52 (0.006)	91.8 (0.121)	97.39 (0.013)	74.37 (0.008)	80.43 (0.015)	85.23 (0.041)	77.27 (0.007)	83.82 (0.025)	92.12 (0.008)
Aug	138.66 (0.003)	135.00 (0.037)	147.87 (0.007)	118.2 (0.002)	122.73 (0.025)	134.66 (0.023)	134.07 (0.0003)	137.51 (0.012)	146.65 (0.006)
Sep	110.44 (0.001)	115.99 (0.023)	116.84 (0.024)	111.36 (0.008)	109.26 (0.04)	122.13 (0.036)	137.34 (0.0003)	138.60 (0.005)	133.56 (0.018)
Oct	104.55 (0.001)	105.52 (0.033)	106.55 (0.008)	107.89 (0.002)	106.98 (0.007)	103.07 (0.051)	98.27 (0.0007)	99.17 (0.003)	97.83 (0.001)
Nov	87.046 (0.005)	90.26 (0.029)	91.62 (0.007)	88.34 (0.006)	90.96 (0.006)	93.42 (0.007)	91.61 (0.004)	89.09 (0.037)	96.50 (0.001)
Dec	75.79 (0.001)	78.08 (0.012)	79.52 (0.005)	75.25 (0.007)	73.33 (0.012)	78.52 (0.01)	80.84 (0.0014)	82.17 (0.006)	85.44 (0.005)
Month	**HOOGLY**			**HOWRAH**			**KALYANI**		
	Present	**Future mid**	**Future late**	**Present**	**Future mid**	**Future late**	**Present**	**Future mid**	**Future late**
Jan	72.59 (0.002)	72.45 (0.005)	76.27 (0.009)	75.99 (0.010)	74.93 (0.006)	78.58 (0.003)	74.02 (0.0006)	74.39 (0.006)	78.17 (0.003)
Feb	84.23 (0.003)	85.18 (0.011)	89.35 (0.016)	85.03 (0.013)	87.32 (0.009)	91.78 (0.0008)	86.52 (0.003)	86.86 (0.009)	91.49 (0.0009)
Mar	131.76 (0.008)	136.78 (0.004)	136.48 (0.0009)	129.81 (0.001)	131.59 (0.004)	134.29 (0.001)	128.76 (0.002)	130.82 (0.005)	133.60 (0.001)
April	129.34 (0.001)	131.98 (0.010)	132.71 (0.022)	133.96 (0.002)	134.58 (0.002)	136.30 (0.0006)	132.97 (0.0009)	134.16 (0.003)	135.94 (0.0008)
May	145.32 (0.001)	146.46 (0.007)	148.19 (0.024)	146.51 (0.004)	148.9 (0.003)	151.51 (0.0008)	146.75 (0.001)	148.32 (0.003)	150.99 (0.0009)
Jun	111.5 (0.002)	110.00 (0.023)	114.18 (0.025)	106.06 (0.002)	108.93 (0.009)	112.89 (0.010)	106.26 (0.003)	109.54 (0.009)	113.2 (0.009)
Jul	75.68 (0.002)	77.96 (0.020)	83.95 (0.024)	84.99 (0.009)	91.88 (0.021)	100.16 (0.007)	86.99 (0.006)	93.16 (0.021)	101.39 (0.007)
Aug	141.57 (0.002)	144.17 (0.022)	151.1 (0.011)	132.18 (0.006)	136.48 (0.010)	144.20 (0.005)	135.5 (0.0003)	138.18 (0.010)	145.52 (0.005)
Sep	131.29 (0.0009)	127.3 (0.012)	127.61 (0.035)	137.78 (0.002)	129.59 (0.004)	132.46 (0.003)	136.48 (0.0002)	128.85 (0.005)	131.82 (0.003)
Oct	92.56 (0.001)	98.75 (0.059)	104.13 (0.048)	96.58 (0.0008)	97.28 (0.003)	103.2 (0.028)	96.28 (0.001)	97.17 (0.003)	102.8 (0.020)
Nov	91.96 (0.005)	80.44 (0.004)	95.92 (0.004)	90.84 (0.005)	93.98 (0.007)	96.16 (0.001)	91.24 (0.005)	94.26 (0.007)	96.44 (0.001)
Dec	79.72 (0.009)	94.29 (0.007)	82.66 (0.011)	79.12 (0.008)	80.39 (0.006)	83.97 (0.006)	78.77 (0.0003)	80.17 (0.006)	83.81 (0.006)

(CV is indicated within parentheses)

TABLE 7

Variation of present and future PET calculated through Makkink's method (RCP 8.5) for different study locations

Month	BOLPUR			BURDWAN			CANNING		
	Present	Future mid	Future late	Present	Future mid	Future late	Present	Future mid	Future late
Jan	64.72 (0.026)	71.63 (0.019)	77.09 (0.01)	70.05 (0.004)	74.15 (0.004)	78.37 (0.017)	74.69 (0.012)	76.95 (0.008)	81.96 (0.007)
Feb	82.08 (0.004)	86.32 (0.003)	87.12 (0.011)	80.07 (0.004)	84.11 (0.018)	86.37 (0.012)	86.38 (0.003)	89.93 (0.008)	98.83 (0.012)
Mar	124.94 (0.002)	130.17 (0.009)	132.68 (0.006)	120.42 (0.012)	131.47 (0.011)	132.9 (0.006)	126.49 (0.002)	129.43 (0.004)	130.59 (0.007)
April	131.89 (0.005)	134.79 (0.026)	145.59 (0.051)	133.58 (0.002)	135.58 (0.007)	139.75 (0.008)	132.95 (0.001)	135.44 (0.004)	140.74 (0.01)
May	133.41 (0.0049)	141.42 (0.013)	145.48 (0.005)	123.36 (0.02)	136.85 (0.032)	130.89 (0.028)	142.10 (0.001)	144.43 (0.004)	148.07 (0.004)
Jun	113.83 (0.052)	109.47 (0.027)	116.39 (0.01)	114.63 (0.039)	113.59 (0.038)	130.51 (0.028)	100.92 (0.003)	105.83 (0.007)	114.21 (0.015)
Jul	91.52 (0.006)	106.08 (0.076)	108.30 (0.043)	74.37 (0.009)	80.78 (0.025)	92.33 (0.052)	77.27 (0.007)	95.09 (0.014)	103.91 (0.031)
Aug	138.66 (0.003)	150.7 (0.034)	142.06 (0.008)	118.20 (0.002)	129.84 (0.027)	123.28 (0.016	134.07 (0.0003)	143.78 (0.009)	149.83 (0.011)
Sep	110.44 (0.001)	112.62 (0.033)	111.58 (0.012)	111.36 (0.001)	106.11 (0.014)	123.26 (0.023)	137.34 (0.0003)	140.1 (0.004)	145.99 (0.009)
Oct	104.55 (0.001)	87.47 (0.056)	97.15 (0.012)	107.89 (0.002)	110.35 (0.003)	100.84 (0.008)	98.23 (0.0007)	96.1 (0.004)	114.44 (0.036)
Nov	87.046 (0.005)	86.63 (0.024)	90.44 (0.01)	88.34 (0.006)	91.48 (0.003)	92.26 (0.052)	91.61 (0.004)	94.91 (0.007)	99.52 (0.005)
Dec	75.79 (0.001)	83.22 (0.012)	84.31 (0.011)	75.25 (0.008)	78.40 (0.021)	83.021 (0.009)	80.84 (0.001)	84.5 (0.006)	88.46 (0.006)
Month	**HOOGLY**			**HOWRAH**			**KALYANI**		
	Present	**Future mid**	**Future late**	**Present**	**Future mid**	**Future late**	**Present**	**Future mid**	**Future late**
Jan	72.59 (0.002)	74.62 (0.018)	78.64 (0.005)	75.99 (0.010)	77.84 (0.008)	83.06 (0.007)	74.025 (0.006)	73.96 (0.008)	79.26 (0.008)
Feb	84.23 (0.003)	87.40 (0.008)	92.48 (0.011)	85.03 (0.012)	87.19 (0.009)	93.43 (0.023)	86.52 (0.003)	87.50 (0.008)	92.41 (0.010)
Mar	131.76 (0.008)	136.98 (0.004)	135.72 (0.006)	129.81 (0.001)	132.24 (0.004)	137.72 (0.006)	128.76 (0.002)	135.93 (0.004)	135.13 (0.008)
April	129.34 (0.001)	131.00 (0.006)	136.56 (0.014)	133.96 (0.002)	133.77 (0.014)	139.30 (0.007)	132.97 (0.009)	130.03 (0.007)	135.43 (0.002)
May	145.32 (0.001)	149.63 (0.008)	152.36 (0.020)	146.51 (0.004)	148.21 (0.004)	153.31 (0.004)	146.75 (0.001)	150.38 (0.002)	159.25 (0.005)
Jun	111.5 (0.002)	111.43 (0.018)	123.11 (0.016)	106.04 (0.002)	110.91 (0.007)	118.48 (0.017)	106.26 (0.003)	112.52 (0.015)	125.62 (0.012)
Jul	75.68 (0.002)	84.23 (0.022)	106.22 (0.056)	84.99 (0.009)	100.23 (0.014)	108.37 (0.023)	86.1 (0.006)	88.58 (0.024)	108.61 (0.038)
Aug	141.57 (0.002)	145.57 (0.009)	155.18 (0.007)	132.18 (0.006)	140.87 (0.008)	149.13 (0.015)	135.5 (0.003)	147.1 (0.006)	153.17 (0.01)
Sep	131.29 (0.0009)	133.52 (0.019)	140.98 (0.015)	137.78 (0.002)	132.29 (0.004)	137.26 (0.012)	136.48 (0.0002)	134.38 (0.014)	140.28 (0.007)
Oct	92.56 (0.001)	100.77 (0.042)	98.74 (0.005)	96.58 (0.008)	103.33 (0.003)	114.27 (0.034)	96.28 (0.001)	99.87 (0.04)	101.45 (0.008)
Nov	91.96 (0.005)	95.55 (0.012)	98.07 (0.003)	90.84 (0.005)	94.26 (0.008)	98.45 (0.006)	91.24 (0.005)	95.73 (0.011)	99.06 (0.005)
Dec	79.72 (0.0009)	81.21 (0.009)	86.46 (0.006)	79.12 (0.008)	83.76 (0.006)	86.1 (0.019)	78.77 (0.003)	81.88 (0.009)	86.43 (0.007)

(CV is indicated within parentheses)

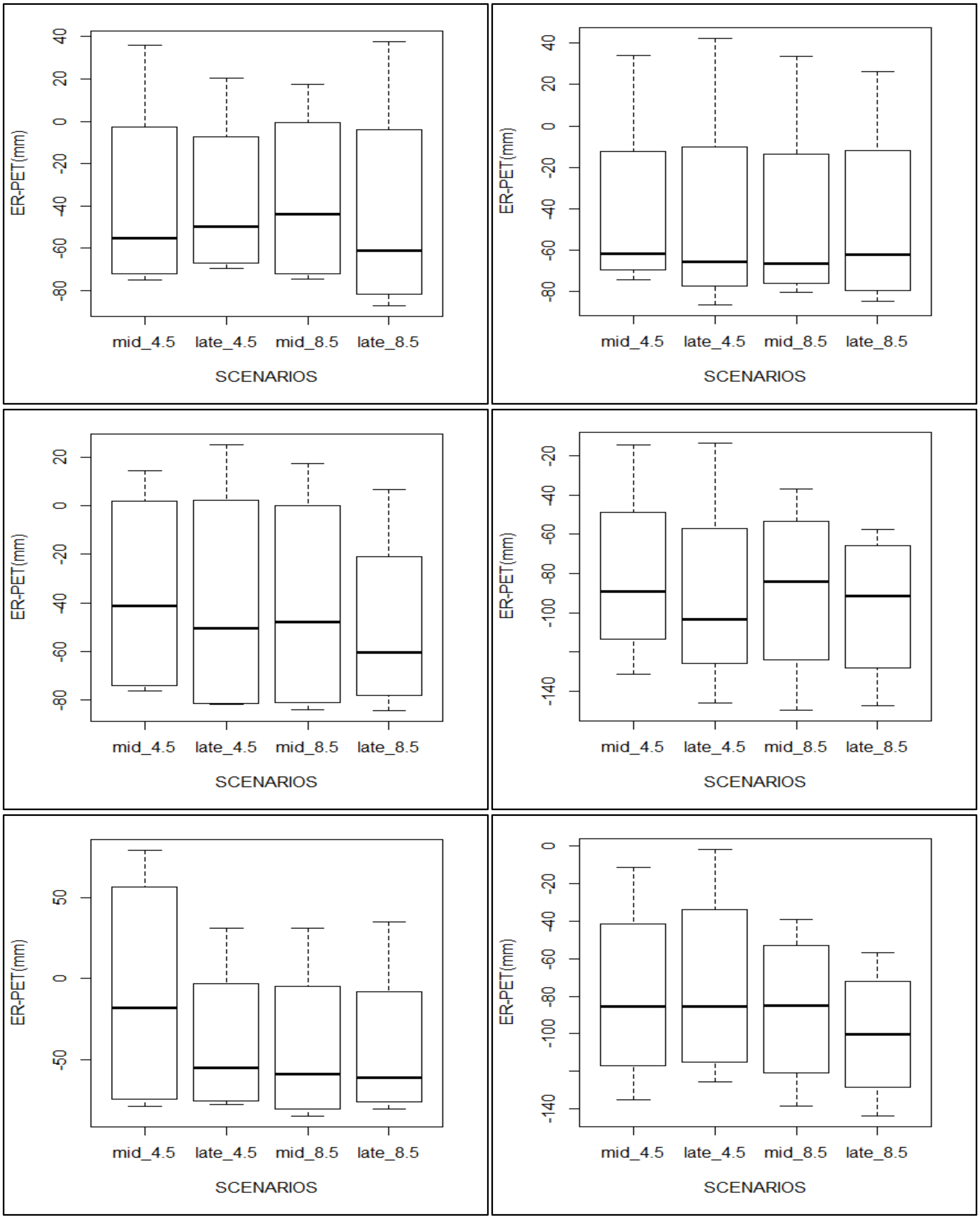

Fig. 4. Seasonal projection of future irrigation requirement (ER-PET) of six stations under study

Monthly trends observed were alike to those in RCP 4.5 (Table 7). January was the month with lowest PET estimate while May showed the highest value (except Burdwan where April records highest PET during end century period). Maximum difference between monthly PET was observed in Kalyani (2070-2090). Burdwan showed the least variation in monthly estimates. Unlike RCP 4.5, no decrease in PET estimate towards end century had been noticed. It was a fairly upward graph with all estimates showed an increasing trend (except Burdwan for the month of October).

4.5. *Comparison of PET values between pre-monsoon and post-monsoon seasons*

The seasons were classified according to India Meteorological Department classification - January and February were taken as winter months; March, April and May comprised as Pre-monsoon / Summer; Monsoon consisted of June, July, August and September; whereas October, November and December were considered as Post-monsoon/Autumn months.

Highest increment in PET throughout the century was projected in Monsoon months, followed by winter and summer season in interchangeable order and finally the lowest rise was witnessed in Autumn season by all three methods in all stations under study. The degree of variation in rise was, however, different for different methods and stations. In Hooghly, the magnitude of rise was similar in all four seasons.The largest variation in PET estimate was shown by Howrah station during monsoon season (~49 mm) by the end of century (as estimated by H/S method). Along with reduction in PET difference between summer and winter months, the annual change in PET has also been diminished to -1mm to 0.5 mm towards the late 2080s. This may be contributed by the fact that temperature rise is also reduced leading to low evapotranspiration.

PET variation throughout the century was different under both scenarios as shown in tables 6 and 7. Overall, a similar upward trend in seasonal PET increment was observed under RCP 8.5, although the increase was largely augmented. Monsoon was the season where PET increase over the century was highest, followed by pre-monsoon (summer) and winter seasons in intermediate places. Post-monsoon (autumn), as usual, showed the least rise in PET value. The largest variation in PET estimate was shown by Hooghly station during monsoon season (111.5 mm) by the end of century, as estimated by Hargreaves Samani method, which was roughly 3.3 times more in RCP 8.5 than in RCP 4.5 scenario. However, a few exceptions could be observed. In case of Bolpur and Burdwan stations, PET estimate in autumn increased minimally in the mid-century period (2030-2050) only to decrease by the end of the century. It was the only season where adecreasing trend had been observed. This was despite the fact that mean temperature was consistently increasing. The estimate in Bolpur was lower for RCP 8.5 than that seen in RCP 4.5. Also, Bolpur was an exception in the regard that summer season surpassed Monsoon in terms of PET increment over the century.

4.6. *Evaluating water availability status through ER and PET*

Many studies reported that alterations in evapotranspiration is a result of precipitation changes (Reynolds *et al*., 2000; Zhang *et al*., 2013; Yang *et al*., 2016;Kundu *et al*., 2017). This relation mainly relied on the tele-connections, air-sea interactions and solar activity (Zhang et al., 2013). It may be noted that fluctuations in rainfall projection was highly erratic and requires more critical analysis than PET.

Knowledge of water availability status by calculating water surplus (wetness) and deficit (dryness) using the water balance equation (ER-PET) is imperative for interpreting the crop water demand along with soil moisture status. The “ER - PET” component (ER: effective rainfall; PET: potential evapotranspiration) gives the net water flux and is a key element of the hydrologic cycle. Fig. 4 showcases boxplot illustrating the projected variability in simulated effective rainfall and potential evapotranspiration (PET) for both mid-century and end-century periods across the selected stations. This comparison provides insights into future irrigation demand by highlighting the potential imbalance between water availability and atmospheric water demand. Makkink method for PET estimation had been used as it showed least deviation with FAO Penman-Monteith [Table 3 and Fig 2]. The combined role of precipitation and PET is helpful in studying the influence of climate change on hydro-climate conditions.

An obvious difference in values between the results estimated by different methods of PET calculation could be noticed; where Makkink overestimated themoisture status, Turc under-estimated the result; HS method gave intermediate output. However, surplus in rainfall was projected to diminish (towards the end century andin RCP 8.5 scenario) which indicated higher irrigation requirement. Compared to the baseline period, all stations showed an enlarged gap (ER-PET) post midcentury. Kalyani is simulated to exhibit highest difference between ER and PET.

Hydrological and climatic extremes in future are results of climate change. In almost all stations, June and July saw an excess of rain, hence no irrigation is recommended during that period. It can be marked that *Kharif* (Monsoon) season gets a surplus of rain in all stations. During this period, pre-*Kharif* rice and jute are the main crops planted. Both being water intensive crops get benefit from the excess rain situation. February, March and April were the months that faces highest water deficit. Therefore, pre-monsoon crops grown in this region heavily depend on irrigation. October also witnessed surplus rain in Bolpur and Canning. Potato is an important winter crop grown in the LGP region. Irrigation is recommended from time to time as per requirement. It must, nevertheless,be noted that midcentury period under RCP 8.5 recorded low water deficiency compared to other period-scenario combinations.

Soil properties affect the water retention capacity of the soil. Bolpur station having red lateritic soil has low water retention capacity. Hence, despite substantial precipitation in the month of June, it faced water deficit (Hargreaves-Samani) (although estimation via Makkink says otherwise). RCP 8.5 exhibited hydrologic extremes - dry periods get drier and wet periods get wetter, particularly by the end century. This extreme weather event is detrimental to crops and needs utmost concern and planning.

It is clear from the figures that under the background of global warming, enhanced evapotranspiration and reduced precipitation towards late century would lead to very high irrigation water demand, mainly under RCP 8.5. The value of “ER - PET” is good indicator of freshwater availability, which shows a declining trend under climate changed scenario.

Crops grown under pre-monsoon in LGP are jute, pre-Kharif (Aus) rice, summer maize, mesta, sesame, groundnut (summer, irrigated) and summer vegetables like cucurbits, etc. Except Aus rice (120-150 cm), the water requirement of other crops (jute, sesame, mesta and groundnut) are around 50 cm. Summer vegetables require about 50 mm of water per week.

The post-monsoon (autumn) season paves the way for Rabi crops. They are sown in autumn (or October) and harvested in spring. Crops grown under this period in LGP are wheat, potatoes, lentils and grams, chickpeas, pigeon peas, rapeseed-mustard having water requirement of 35 cm, 32 cm, 24 cm, 25 cm, 60 cm, and 50 cm, respectively (Biswas *et al*., 2006).

The increasing irrigation application rate will definitely take a toll on total farm economics. Thus, the economic use of water to ensure a profitable return is mandatory. Not all irrigation sources are cost-effective and give the same economic return, and hence ensuring a profitable venture, keeping in mind optimum crop yield, is encouraged. Surface irrigation is the most widely used method and has an application efficiency of 60% (Abou Zeid, 2002).

Projected climate has shown that the inclination to irrigated crop production will be dominant in all traditionally rainfed production regions. Demand on farmers’ use of irrigation water is predicted to be a direct result of the use of irrigation water as an economic input for crop production (Xu *et al*., 2019). Water deficit [as suggested by negative values of ‘ER-PET’ (Fig. 4)] is more in the case of pre-monsoon season than post-monsoon season. However, the crops grown during pre-monsoon have a higher water requirement. If we grow wheat, lentil, gram, and mustard in post-monsoon season, the pressure on surface and groundwater storage will be less. The farmers who choose to grow two crops per year are also encouraged to take up post-monsoon crops so that the total irrigation requirement will be less.

7. Conclusion

Climate change has a direct impact on agricultural production. Alterations in hydrologic events lead to unprecedented changes in crop water requirement pattern. Sound knowledge of hydrologic processes helps in accurate planning of irrigation, enhancing water utilization by plants and minimizing wastage, leading to sustainable crop yields and improvement in water productivity. The pattern of changes in various climatic variables has been duly investigated to estimate the long-term water resources of the region. Temperature – both minimum and maximum, show an increase over time and is expected to reach maximum by late century period under the RCP 8.5 scenario. Highest mean temperature rise (by almost 3.5 °C) has been simulated for Kalyani (late RCP 8.5 scenario) for pre-monsoon period [when comparing Tables 4A and 4B]. Least impact of global temperature rise has been observed in Canning. PET increase is substantial in all stations and scenarios; a higher increase is evidently seen during monsoon months. All six stations exhibit dissimilar pattern of variation. Maximum PET growth under RCP 4.5 scenario has been observed in Howrah. Under RCP 8.5 scenario, Canning shows highest PET. Although projected daily mean temperature is low, enhanced PET is a result of high solar radiation. High PET is detrimental to soils of sodic origin due to heavy accumulation of salts that hamper plant growth. January is consistently the month with lowest PET while highest is predicted in May. Increased PET generally results in shortening of crop growth period. Crop growth pattern is also expected to be altered based on the resultant meteorological conditions by the end of the century. Makkink method showed the least variation throughout the century in all stations and scenarios.

Although an overall increase in rainfall (5-6.8%) is estimated for RCP 4.5 scenario, rainfall tends to decrease under RCP 8.5. Kalyani shows maximum decline in precipitation (22.8%). Rainfall estimates are quite unsteady throughout the future scenario. The trend of increase is not uniform with episodes of increase and decrease within decades under both scenarios for all stations under study. The wet months get wetter and dry months get drier leading to many possible flood and drought periods, adhering to Chao *et al*. (2013), Murray-Tortarolo *et al*. (2016) and Mallakpour *et al*. (2018). Excess rain during monsoon months compensates for excessive ET losses during the season and hence irrigation is not recommended then. However, during other months a negative 'ER-PET' value is seen which suggests the requirement of irrigation. Data comparison with FAO PM method shows that in a data-scarce situation as seen in this study, it might be feasible to make hydrological projections and therefore, such projections are useful in efficient crop planning. Results indicate a higher possibility of water shortage for Kalyani and Hoogly in late_8.5 scenario and adaption measures assist in mitigating the effects of substantial drought in crop production.

Data availability

All the data used in this study is available on request

Acknowledgment and funding

We acknowledge the financial support provided by the Department of Science and Technology (DST), Government of India, through the Inspire Fellowship program.

Authors' contributions

Abhilashaa Das: Data collection, analysis and writing. (Email- das.abhilashaa@bckv.edu.in)
Saon Banerjee: Conceptualization, writing and editing
Sarathi Saha: Reviewing and writing(Email-sarathisaha94@gmail.com).

Disclaimer: The contents and views presented in this research article/paper are the views of the authors and do not necessarily reflect the views of the organizations they belong to.

References

Abou Zeid, K., 2002, "Egypt and the world water goals", Egypt statement in the World Summit for sustainable development and beyond, Johannesburg.

Allen, R. G., Pereira, L. S., Raes, D., and Smith, M., 1998, "Crop Evapotranspiration: Guidelines for Computing Crop Water Requirements", *FAO Irrigation and Drainage Paper*, FAO, Rome, 300 p.

Asanuma, and Kamimera, H., 2004, "Long-term trend of pan evaporation measurements in Japan and its relevance to the variability of the hydrological cycle", in Proceedings of the Symposium on Water Resource and its Variability in Asia, Meteorological Research Institute, Tsukuba, Japan, March 2004.

Bae, D. H., Jung, I. W., and Lettenmaier, D. P., 2011, "Hydrologic uncertainties in climate change from IPCC AR4 GCM simulations of the Chungju Basin, Korea", *Journal of Hydrology*, **401**, 1-2, 90-105.

Banerjee, S., and Biswas, B., 2020, "Assessing Climate Change Impact on Future Reference Evapotranspiration Pattern of West Bengal, India", *Agricultural Sciences*, **11**, 9, 793-802.

Biswas, B., Ghosh, D. C., Dasgupta, M. K., Trivedi, N., Timsina, J., and Dobermann, A., 2006, "Integrated assessment of cropping systems in the Eastern Indo-Gangetic plain", *Field Crops Research*, **99**, 1, 35-47.

Burn, N. and Hesch, N. M., 2007, "Trends in evaporation for the Canadian Prairies", *Journal of Hydrology*, **336**, 1, 61–73.

Carter, T.R., Parry, M.L., Harasawa, H., and Nishioka, S., 1994, "IPCC Technical Guidelines for Assessing Climate Change Impacts and Adaptations", IPCC Special Report to Working Group II of IPCC, London: University College London, and Tsukuba, Japan: Centre for Global Environmental Research.

Chandran, M. A. S., Banerjee, S., Mukherjee, A., Nanda, M. K., and Kumari, V. V., 2022, "Evaluating the long-term impact of projected climate on rice-lentil-groundnut cropping system in Lower Gangetic Plain of India using crop simulation modeling", *International Journal of Biometeorology*, **234**, 1-15.

Chattopadhyay, N. and Hulme, M., 1997, "Evaporation and potential evapotranspiration in India under conditions of recent and future climate change", *Agricultural and Forest Meteorology*, **87**, 1, 55–73.

Chen, H., Xu, C. Y., and Guo, S., 2012, "Comparison and evaluation of multiple GCMs, statistical downscaling and hydrological models in the study of climate change impacts on runoff", *Journal of Hydrology*, **434**, 36-45.

Claessens, L., Antle, J. M., Stoorvogel, J. J., Valdivia, R. O., Thornton, P. K., and Herrero, M., 2012, "A method for evaluating climate change adaptation strategies for small-scale farmers using survey, experimental and modeled data", *Agricultural Systems*, **111**, 85-95.

Collins, W. J., Bellouin, N., Doutriaux-Boucher, M., Gedney, N., Halloran, P., Hinton, T., and Woodward, S., 2011, "Development and evaluation of an Earth-System model–HadGEM2", *Geoscientific Model Development*, **4**, 4, 1051-1075.

Das, L., Javed Akhter, M.D. and Acharya, S.K., 2020, "Future Monsoon Rain over Gangetic West Bengal Simulated by CMIP5 GCMs", *Atmosphere*, **20**, p.50.

Debnath, J., Sahariah, D., Mazumdar, M., Lahon, D., Meraj, G., Hashimoto, S., Kumar, P., Singh, S.K., Kanga, S., Chand, K. and Saikia, A., 2023, "Evaluating flood susceptibility in the brahmaputra river basin: an insight into Asia's Eastern Himalayan floodplains using machine learning and multi-criteria decision-making", *Earth Systems and Environment*, **7**, 4, 733-760.

Debnath, S., Adamala, S. and Raghuwanshi, N.S., 2015, "Sensitivity analysis of FAO-56 Penman-Monteith method for different agro-ecological regions of India", *Environmental Processes*, **2**, 4, 689-704.

Delghandi, M., Joorabloo, S., and Emamgholizadeh, S., 2017, "Climate change impacts on spatial-temporal variations of reference evapotranspiration in Iran", *Water Harvesting Research*, **2**, 1, 13-23.

Dong, N., Yu, Z., Gu, H., Yang, C., Yang, M., Wei, J., Wang, H., Arnault, J., Laux, P., and Kunstmann, H., 2019a, "Climate-induced hydrological impact mitigated by a high-density reservoir network in the Poyang Lake Basin", *Journal of Hydrology*, **579**, 124148.

Dong, Y., Proistosescu, C., Armour, K. C., and Battisti, D. S., 2019b, "Attributing historical and future evolution of radiative feedbacks to regional warming patterns using Green's function approach: The preeminence of the western Pacific", *Journal of Climate*, **32**, 17, 5471-5491.

Dunne, J. P., John, J. G., Adcroft, A. J., Griffies, S. M., Hallberg, R. W., Shevliakova, E., Stouffer, R. J., Cooke, W., Dunne, K. A., Harrison, M. J., Krasting, J. P., and Zadeh, N., 2012, "GFDL's ESM2 global coupled climate–carbon earth system models. Part I: Physical formulation and baseline simulation characteristics", *Journal of Climate*, **25**, 19, 6646-6665.

Giménez, P. O., and García-Galiano, S. G., 2018, "Assessing regional climate models (RCMs) ensemble-driven reference evapotranspiration over Spain", *Water*, **10,** 9, 1181.

Hargreaves, G. H., and Samani, Z. A., 1985, "Reference crop evapotranspiration from temperature", *Applied Engineering in Agriculture*, **1,** 2, 96-99.

Hinrichsen, D., and Tacio, H., 2002, "The coming freshwater crisis is already here. The linkages between population and water", Washington, DC: Woodrow Wilson International Center for Scholars, **43**, 1-26

Hobbins, J. A., Ramírez, and T. C. Brown, 2004, "Trends in pan evaporation and actual evapotranspiration across the conterminous U.S.: paradoxical or complementary?", *Geophysical Research Letters*, **31**, 13, 13503.

Huo, Z., Dai, X., Feng, S., Kang, S., and Huang, G., 2013, "Effect of climate change on reference evapotranspiration and aridity index in arid region of China", *Journal of Hydrology*, **492**, 24-34.

Idso, S. B., Jackson, R. D., and Reginato, R. J., 1975, "Estimating evaporation: a technique adaptable to remote sensing", *Science*, **189**, 4207, 991-992.

IPCC, 2013, "Climate Change: The Physical Science Basis", *Contribution of Working Group I to the Fifth Assessment Report of the Intergovernmental Panel on Climate Change*. Cambridge University Press: Cambridge, UK.

Jones, P. G., and Thornton, P. K., 2003, "The potential impacts of climate change on maize production in Africa and Latin America in 2055", *Global Environmental Change*, **13**, 1, 51-59.

Jones, P. G., and Thornton, P. K., 2013, "Generating downscaled weather data from a suite of climate models for agricultural modelling applications", *Agricultural Systems*, **114**, 1-5.

Kundu, S., Khare, D., and Mondal, A., 2017, "Future changes in rainfall, temperature and reference evapotranspiration in central India by least square support vector machine", *Geoscience Frontiers*, **8**, 3, 583–596.

Makkink, G.F., 1957, "Testing the Penman formula by means of lysimeters", *Journal of the Institution of Water Engineering*, **11**, 3, 277-288.

Mallakpour, I., Sadegh, M., and Agha Kouchak, A., 2018, "A new normal for streamflow in California in a warming climate: Wetter wet seasons and drier dry seasons", *Journal of Hydrology*, **567**, 203-211.

Mallik, P. and Ghosh, T., 2022, "Impact of climate on tea production: a study of the Dooars region in India", *Theoretical and Applied Climatology*, **147**, 1, pp.559-573.

Mavromatis, T., and Hansen, J. W., 2001, "Interannual variability characteristics and simulated crop response of four stochastic weather generators", *Agricultural and Forest Meteorology*, **109**, 4, 283-296.

Moratiel, R., Snyder, R. L., Durán, J. M., and Tarquis, A. M., 2011, "Trends in climatic variables and future reference evapotranspiration in Duero Valley (Spain)", *Natural Hazards and Earth System Sciences*, **11,** 6, 1795-1805.

Murray-Tortarolo, G., Friedlingstein, P., Sitch, S., Seneviratne, S. I., Fletcher, I., Mueller, B., and Zeng, N., 2016, "The dry season intensity as a key driver of NPP trends", *Geophysical Research Letters*, **43,** 6, 2632-2639.

Ndiaye, P. M., Bodian, A., Diop, L., Dezetter, A., Guilpart, E., Deme, A., and Ogilvie, A., 2021, "Future trend and sensitivity analysis of evapotranspiration in the Senegal River Basin", *Journal of Hydrology: Regional Studies*, **35**, 100820.

Obreza, T. A., and Pitts, D. J., 2002, "Effective rainfall in poorly drained micro-irrigated citrus orchards", *Soil Science Society of America Journal*, **66**, 1, 212-221.

Ouhamdouch, S., Bahir, M., Ouazar, D., Goumih, A., and Zouari, K., 2020, "Assessment of the climate change impact on future evapotranspiration and flows from a semi-arid environment", *Arabian Journal of Geosciences*, **13,** 2, 1-14.

Pan, S., Tian, H., Dangal, S. R., Yang, Q., Yang, J., Lu, C., Tao, B., Ren, W., and Ouyang, Z., 2015, "Responses of global terrestrial evapotranspiration to climate change and increasing atmospheric CO_2 in the 21st century", *Earth's Future*, **3**, 1, 15-35.

Papaioannou, G., Kitsara, and N. Melanitis, 2007, "Temporal analysis of hydrometeorological characteristics in Crete", in *Proceedings of the Symposium on Water Resources Management: New Approaches and Technologies (EWRA '07)*, Chania, Greece.

Reynolds, J. F., Kemp, P. R., and Tenhunen, J. D., 2000, "Effects of long-term rainfall variability on evapotranspiration and soil water distribution in the Chihuahuan Desert: a modeling analysis", *Plant Ecology*, **150**, 1, 145-159.

Roderick, M. L., and G. D. Farquhar, 2002, "The cause of decreased pan evaporation over the past 50 years", *Science*, **298**, 5597, 1410–1411.

Samani, Z., 2000, "Estimating solar radiation and evapotranspiration using minimum climatological data", *Journal of Irrigation and Drainage Engineering*, **126**, 4, 265-267.

Scheff, J., and Frierson, D. M., 2014, "Scaling potential evapotranspiration with greenhouse warming", *Journal of Climate*, **27,** 4, 1539–1558.

Seiller, G., and Anctil, F., 2016, "How do potential evapotranspiration formulas influence hydrological projections", *Hydrological Sciences Journal*, **61**, 12, 2249-2266.

Shamir, E., Mendoza Fierro, L., Mohsenzadeh Karimi, S., Pelak, N., Tarouilly, E., Chang, H.I. and Castro, C.L., 2024, "Climate Change Projections of Potential Evapotranspiration for the North American Monsoon Region", *Hydrology*, ***11***, 6, p.83.

Shi, X., Mao, J., Thornton, P. E., and Huang, M., 2013, "Spatiotemporal patterns of evapotranspiration in response to multiple environmental factors simulated by the Community Land Model", *Environmental Research Letters*, **8**, 2, 024012.

Sirohi, N. P. S., 1989, "Long-term Strategies and Programmes for Mechanization of Agriculture in Agro Climatic Zone–III: Lower Gangetic Plains region", Indian Planning Commission, Government of India.

Sperna Weiland, F. C., Van Beek, L. P. H., Kwadijk, J. C. J., and Bierkens, M. F. P., 2012, "Global patterns of change in discharge regimes for 2100", *Hydrology and Earth System Sciences*, **16**, 4, 1047-1062.

Srinivasa Raju, K., Sonali, P., and Nagesh Kumar, D., 2017, "Ranking of CMIP5-based global climate models for India using compromise programming", *Theoretical and Applied Climatology*, **128**(3-4), 563-574.

Srinivasa Raju, K., and Nagesh Kumar, D., 2015, "Ranking general circulation models for India using TOPSIS", *Journal of Water and Climate Change*, **6**(2), 288-299.

Su, Z., 2002, "The Surface Energy Balance System (SEBS) for estimation of turbulent heat fluxes", *Hydrology and Earth System Sciences*, **6**, 1, 85-100.

Taylor, K. E., Stouffer, R. J., and Meehl, G. A., 2012, "An overview of CMIP5 and the experiment design", *Bulletin of the American Meteorological Society*, **93**, 4, 485-498.

Tebakari, J., Yoshitani, and C. Suvanpimol, 2005, "Time-space trend analysis in pan evaporation over Kingdom of Thailand", *Journal of Hydrologic Engineering* **10**, 3, 205–215.

Thornton, P. K., Jones, P. G., Alagarswamy, G., & Andresen, J., 2009, "Spatial variation of crop yield response to climate change in East Africa", *Global environmental change*, **19**, 1, 54-65.

Trotochaud, J., Flanagan, D. C., and Engel, B. A., 2016, "A simple technique for obtaining future climate data inputs for natural resource models", *Applied Engineering in Agriculture*, **32**, 3, 371-381.

Turc, L., 1961, "Estimation of irrigation water requirements, potential evapotranspiration: A simple climatic formula evolved up to date", *Annals of Agronomy*, **12**, 13-14.

Watanabe, M., Suzuki, T., O'ishi, R., Komuro, Y., Watanabe, S., Emori, S., Takemura, T., Chikira, M., Ogura, T., Sekiguchi, M., and Kimoto, M., 2010, "Improved climate simulation by MIROC5: Mean states, variability, and climate sensitivity", *Journal of Climate*, **23**, 23, 6312-6335.

Wigley, T. M. L., Jones, P. D., Briffa, K. R., and Smith, G., 1990, "Obtaining sub-grid-scale information from coarse-resolution general circulation model output", *Journal of Geophysical Research: Atmospheres*, **95**, D2, 1943-1953.

Xu, Q., Fox, G., McKenney, D., and Parkin, G., 2019, "A theoretical economic model of the demand for irrigation water", *Agricultural Water Management*, **225**, 105763.

Yang, Y., Anderson, M., Gao, F., Hain, C., Noormets, A., Sun, G., ... and Sun, L., 2020, "Investigating impacts of drought and disturbance on evapotranspiration over a forested landscape in North Carolina, USA using high spatiotemporal resolution remotely sensed data", *Remote Sensing of Environment*, **238**, 111018.

Yang, Z., Qiang Zhang, and Xiaocui Hao, 2016, "Evapotranspiration Trend and Its Relationship with Precipitation over the Loess Plateau during the Last Three Decades", *Agricultural Water Management*, **95**, 707–715.

Yuan, X., and Bai, J., 2018, "Future projected Changes in Local evapotranspiration Coupled with Temperature and precipitation variation", *Sustainability*, **10,** 9, 3281.

Zhang, D., Liu, X., and Hong, H., 2013, "Assessing the effect of climate change on reference evapotranspiration in China", *Stochastic Environmental Research and Risk Assessment*, **27**, 8, 1871-1881.